ISBN: 978-3-95450-192-2 doi:10.18429/JACoW-IBIC2017-MO3AB1

CHARACTERIZING THE COUPLED BUNCH DRIVING TERMS IN A STORAGE RING *

Katherine C. Harkay†, Tim Berenc, Louis Emery, Ulrich Wienands, ANL, Argonne, IL, USA
Dmitry Teytelman, Dimtel, Inc., San Jose, CA, USA
John Byrd, LBNL, Berkeley, CA, USA
Rohan Dowd, Australian Synchrotron, Clayton, Australia

Abstract

Stable operation of a modern high current storage rings requires attention to the sources of coupling impedance. Methods ranging from EM modeling to bench and beam measurements are routinely used to characterize accelerator components. The beam-based method presented here complements existing approaches, and allows precise measurements and identification of narrowband resonances in structures such as RF cavities or in-vacuum undulators. We combine the well-established approach of characterizing eigenvalues of coupled-bunch instabilities with modern high-throughput data acquisition tools and automatic analysis methods. By sequentially exciting low-amplitude oscillation of individual modes below the instability threshold and observing open-loop damping, we automatically map the eigenvalues of all even-fill eigenmodes. Repeating the measurements while changing operating conditions, such as cavity temperatures or undulator gaps, provides a detailed mapping of the impedance source. These measurements are used to extract impedance parameters as well as to optimize accelerator settings. Experimental results from the Advanced Photon Source and other accelerators illustrate the technique.

INTRODUCTION

In this paper we present a beam-based method for measuring narrowband coupling impedances in a storage ring. Such narrow resonant modes, typically parasitic modes in vacuum structures or higher-order modes (HOMs) in RF cavities, can potentially excite severe coupled-bunch instabilities. Precise characterization of these resonances is important for optimizing the operation of existing machines as well as for planning of upgrades.

MEASUREMENT METHOD

Instabilities and Impedances

In order to characterize the coupling impedances we measure the eigenvalues of the even-fill eigenmodes (EFEMs). Modal eigenvalue Λ_l defines the open-loop trajectory $A_l e^{\Lambda_l t}$ of EFEM l. The real part of the eigenvalue determines the modal growth or damping rate and the imaginary part — the oscillation frequency. In the longitudinal plane, the eigenvalues are described by the following relation:

$$\Lambda_l = \Lambda_0 + \frac{\pi\alpha e f_{\rm rf}^2 I_0}{E_0 h\omega_s} Z^{\parallel\rm eff}(l\omega_0 + \omega_s), \qquad (1)$$

where $\Lambda_0 = -\lambda_{\rm rad} + i\omega_s$ is the unperturbed eigenvalue, $Z^{\parallel\rm eff}$ is the effective impedance, related to the physical impedance as follows:

$$Z^{\parallel\rm eff}(\omega) = \sum_{p=-\infty}^{\infty} \frac{p\omega_{\rm rf} + \omega}{\omega_{\rm rf}} Z^{\parallel}(p\omega_{\rm rf} + \omega) \qquad (2)$$

In the transverse plane we have [1]:

$$\Lambda_l = (-\lambda_{\rm rad}^{\perp} + i\omega_\beta) - \frac{cef_{\rm rev} I_0}{2\omega_\beta E_0} Z^{\perp\rm eff}(l\omega_0 + \omega_\beta) \qquad (3)$$

$$Z^{\perp\rm eff}(\omega) = \sum_{p=-\infty}^{\infty} Z^{\perp}(p\omega_{\rm rf} + \omega), \qquad (4)$$

where c is the speed of light and ω_β is the betatron frequency. The transverse impedance, unlike longitudinal, does not scale with frequency when aliasing to $Z^{\perp\rm eff}$.

Modal eigenvalues sample machine impedances at synchrotron or betatron sidebands of many revolution harmonics. To characterize the resonant modes we need a way to tune their frequencies. For higher order modes in RF cavities the typical method for tuning the HOMs is to change the cavity temperature. Mechanisms to change the geometry of the structure provide another way of tuning the resonances. These include cavity tuners, in-vacuum undulators (IVUs) with movable jaws, and others.

A measurement of complex eigenvalues as a function of a tuning parameter characterizes the aliased effective impedance $Z^{\rm eff}(\omega)$. In order to reconstruct the original HOM resonance additional information is required. Aliased impedance measurement defines, with the resolution of the RF frequency, where in the spectrum the true impedance might be located. One way to localize the impedance is to compare these frequencies to the known HOM spectra, from simulations or bench measurements. If the structure in question has RF probes, it can be investigated with beam to resolve various resonances. In this case, a single-bunch fill pattern is normally used to generate a comb of revolution frequency harmonics extending beyond the beam pipe cut-off frequency.

To summarize, by scanning a resonant mode and measuring EFEM eigenvalues we can extract the response as a function of the scanning parameter. In order to translate that information to the modal frequency and bandwidth we need

* Work at supported by U. S. Department of Energy, Office of Science, under Contract No. DE-AC02-06CH11357.
† harkay@aps.anl.gov

ISBN: 978-3-95450-192-2 doi:10.18429/JACoW-IBIC2017-MO3AB1

two pieces of information — the conversion factor/function between the scanning parameter and HOM frequency and the original unaliased frequency of the HOM. In some situations we can obtain the conversion factor by observing the effect of the single HOM on multiple EFEMs. As the Advanced Photon Source (APS) measurements demonstrate, when the resonances have very high Q, their tuning can be extracted from the eigenvalue shifts of closely spaced synchrotron sidebands with $2f_s$ separation. In the transverse plane, closest sidebands are spaced by twice the fractional betatron tune[1]. In other situations, tuning sensitivity can be high enough to move the mode across several revolution harmonics, thus providing a convenient calibration — this is the approach taken in the Australian Synchrotron measurements.

Unfortunately, there is no universal recipe for extracting impedance parameters. In each case, a unique combination of impedance sources, accelerator parameters, and physically accessible controls and measurement signals determines what can and cannot be characterized. Thus, experimenters should be ready to improvise and to adapt the measurement to the machine.

Experimental Setup

Our method is based on the transient drive/damp measurement. In this measurement, a bunch-by-bunch feedback system is configured to excite a single eigenmode with sinusoidal output. Upon a software trigger, the excitation is turned off and the evolution of the eigenmode is recorded in the open loop configuration. The drive/damp measurement dates from the mid-1990s [2], [3, page 47]. In general, this measurement can be performed both below and above the instability threshold. Since the feedback is turned off for all EFEMs, it is easier to perform the measurements under the threshold. Above the instability threshold, unstable modes grow exponentially, limiting the maximum allowable time in the open-loop state. This limit interferes with measurements of slowly damping EFEMs.

An important advantage of the drive/damp measurement over the traditional grow/damp measurement performed above the instability threshold is that any eigenmode can be probed at will. As discussed below, measurements of stable eigenmodes shifted to faster damping by the HOMs are important for proper characterization of unaliased impedances.

While the measurement technique was first utilized in the early 1990s, recent advances in real-time data acquisition capabilities and online/offline analysis have pushed the method to a qualitatively new state. Modern diagnostic systems allow measurement of more than one or two modes —an arbitrary subset or even all eigenmodes can be quickly scanned. This extension of the approach was first developed at Diamond Light Source [4] and has been since used at multiple accelerators around the world.

With a large number of eigenmodes to probe, efficient data acquisition is critical. THe feedback processor used in these experiments (iGp12) captures 20–35 ms of beam motion every 500 ms. The repetition rate is limited by the internal memory readout bandwidth of 320 Mbps. Using a custom mode scan tool we streamed these acquisitions to a control computer. The mode scan tool steps the drive excitation frequency through a range of eigenmodes, specified by the user, and captures a desired number of measurements for each mode.

Data sets, captured as described in the previous section, are automatically processed by our custom Matlab tools to extract the modal eigenvalues (growth or damping rates and oscillation frequencies). The traditional approach to analyzing bunch-by-bunch data is to transform signals from bunch to EFEM basis [5]. Such analysis is powerful, since it extracts all the eigenmodes, but is computationally intensive. If, however, we are only interested in a single eigenmode, a much more efficient approach is available. In this method, we select the appropriate single detection frequency for the eigenmode in question[2], mix the beam signal with the complex exponential reference signal $e^{i\omega t}$, and lowpass filter the result. This process shifts the desired mode to baseband and lowpass filtering selects only that eigenmode. THe resulting complex trajectory is then fitted with a complex exponential to estimate the growth/damping rate and the oscillation frequency. For a detailed discussion of the eigenvalue estimation method refer to [3, pages 48–54].

Limitations

We would be remiss not to discuss the limitations of the technique described here. As discussed earlier, measuring EFEM eigenvalues under the instability threshold allows the experimenter to extend the feedback-off period as far as needed, in order to resolve very long damping times. At the same time, the eigenvalue shift from a given impedance scales linearly with beam current, thus limiting sensitivity to smaller impedances.

Another important limitation is due to the fact that we characterize the impedances by measuring eigenvalue shifts. If the unperturbed eigenvalue Λ_0 changes from measurement to measurement, it limits the smallest resolvable shifts. This effect is most pronounced in the transverse plane, specifically, in the EFEM frequency measurements.

EXPERIMENTAL RESULTS

In this work we present results of three experimental measurements at three different accelerators: longitudinal at MAX IV 3 GeV ring, vertical at the Australian Synchrotron (AS), and longitudinal at the Advanced Photon Source (APS). The measurements are arranged in increasing order of sophistication in the experimental technique. At MAX IV, measurements of a single eigenmode were performed above the instability threshold. This approach is conceptually identical to the work presented in [6]. In the AS studies, a group of vertical EFEMs was measured both below and above the threshold. Finally, at the APS, complete modal scans

[1] Closest spacing is $2\omega_\beta - \omega_{\rm rev}$ for $\omega_\beta > \omega_{\rm rev}/2$.

[2] Upper or lower synchrotron sideband of the appropriate revolution harmonic.

ISBN: 978-3-95450-192-2 doi:10.18429/JACoW-IBIC2017-MO3AB1

Table 1: MAX IV Parameters

Parameter description	Value
Beam energy	3 GeV
Beam current	500 mA
Number of bunches	176
Nominal RF frequency	100 MHz
Harmonic number	176
Synchrotron frequency	680 Hz
Radiation damping time	25 ms

Table 2: AS Parameters

Parameter description	Value
Beam energy	3 GeV
Beam current	200 mA
Number of bunches	300
Nominal RF frequency	499.654 MHz
Harmonic number	360
Vertical tune	5.216

below the instability threshold were used to identify and characterize multiple longitudinal HOMs in RF cavities.

MAX IV 3 GeV

Relevant parameters of the MAX IV 3 GeV ring are summarized in Table 1. The goal of longitudinal instability studies in MAX IV was to optimize cavity temperatures for minimum growth rates. Before temperature optimization the longitudinal instability threshold was 3 mA. With an low shunt impedance improvised kicker [7], reduction of growth rates was necessary to extend the control range of the longitudinal feedback.

Figure 1 shows the result of a temperature scan of the main RF cavity 20, with the eigenvalues of mode 167 responding to the temperature changes. In order to quantify

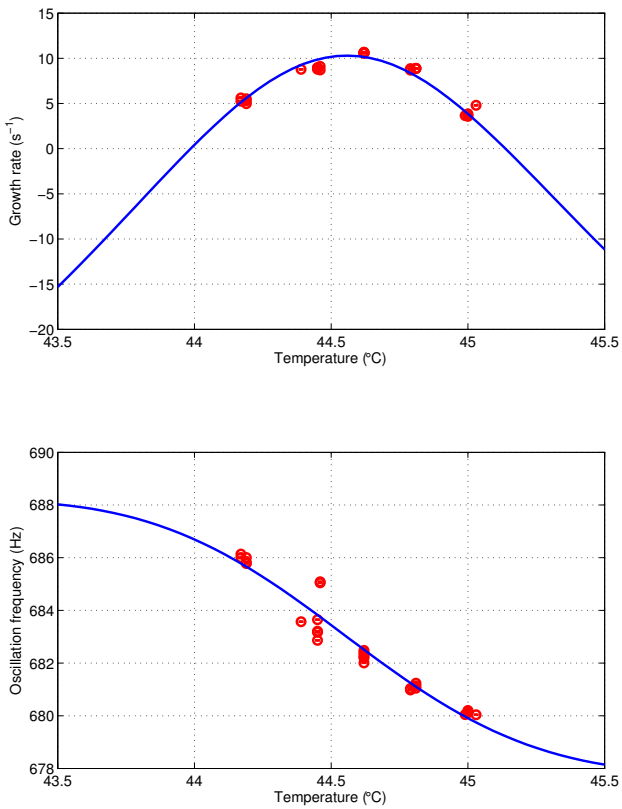

Figure 1: Mode 167 eigenvalues and the resonant fit.

the effective impedance we fit a resonant mode response to the measurements.

The most straightforward analysis technique is to fit resonant responses to the measured modal eigenvalues using temperature as a substitute for frequency. At each temperature T the eigenvalue can be calculated using the following five-parameter form:

$$\lambda = \frac{i\lambda_{\max} T T_{\mathrm{bw}}}{T_0^2 + iTT_{\mathrm{bw}} - T^2} + \lambda_0 + i\omega_s^0 \qquad (5)$$

where T_0 is the temperature where peak growth rate $\lambda_{\max}$ is reached, T_{bw} is the resonant bandwidth, λ_0 is baseline growth rate[3] and ω_s^0 is the base modal frequency[4].

After similar temperature scans were performed on all main and harmonic RF cavities, we adjusted the cavity temperatures to minimize the growth rates, increasing the longitudinal instability threshold from 3 to 17 mA.

Australian Synchrotron

In the Australian Synchrotron, fast vertical growth rates are observed, driven by the IVUs. When the IVU gaps are open, vertical instabilities are dominated by the resistive wall. When the gaps are closed, however, much faster instabilities occur. The growth rates of these instabilities depend strongly on the gap position. Figure 2 shows the growth rates for mode 359 (−1, resistive wall) and 222–224 as a function of IVU05 gap setting. As the gap is reduced, the resonant mode crosses the lower betatron sideband of 222$^{\mathrm{nd}}$ revolution harmonic, then 223$^{\mathrm{rd}}$ and 224$^{\mathrm{th}}$. Of course, these can be baseband harmonics or harmonics above any multiple of the RF frequency.

Fitting resonant responses to the growth rates of individual modes we generate the plot shown in Fig. 3, this time using the IVU gap as a substitute for frequency. Spacing of the peaks for the neighboring modes corresponds to the resonance shifting by ω_{rev} and provides a convenient way to calibrate our scanning parameter. Two distances agree within 3% and give us the tuning coefficient of 4.8 MHz mm^{-1}. Fitted bandwidths range from 75 to 78 µm or 360–374 kHz. The fits show that the shunt impedance increases as the undulator jaws get closer to the beam.

[3] Radiation damping rate is expected here, unless constant impedances due to cavities in other regions are shifting the eigenvalue.

[4] Should be the zero current synchrotron frequency without other impedances affecting the eigenmode.

ISBN: 978-3-95450-192-2 doi:10.18429/JACoW-IBIC2017-MO3AB1

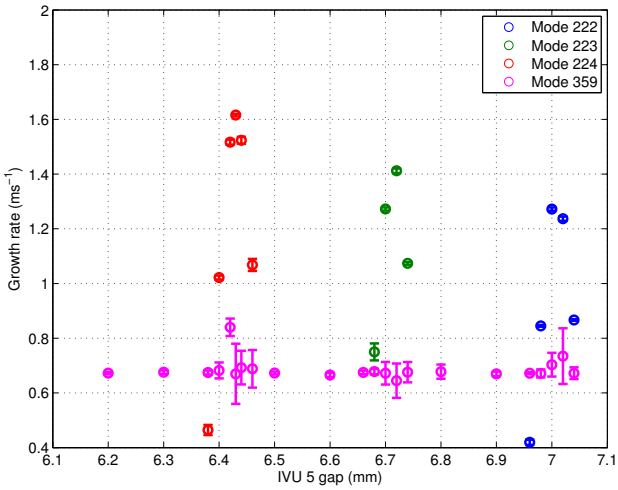

Figure 2: Vertical growth rates vs. IVU05 gap setting.

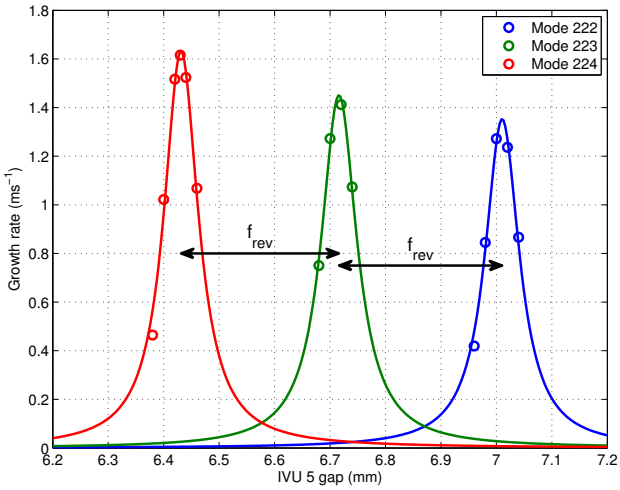

Figure 3: Vertical growth rates and resonant mode fits.

Unlike cavity HOM tuning, IVU jaws do have to travel through the resonant region, so the instability cannot be fully avoided. At the same time, these measurements can be used in operation to select more stable positions and to add stability when the resonant mode crosses the betatron sideband[5].

A numerical study of resonant modes in IVU05 was done using HFSS [8]. Table 3 compares calculated and measured parameters. In general, we see good agreement between these, taking into consideration the fact that HFSS model assumed ideal electrical conductivities for all materials and, therefore, under-estimated the bandwidth.

[5] Additional stabilization can come from the increased bunch-by-bunch feedback gain or from raised chromaticity. Both of these have negative side effects and are best kept lower in steady state operation.

Table 3: Comparison of Measured and Modeled Parameters for the IVU05 Mode 3

Parameter description	Measurement	Model
Tuning sensitivity, MHz mm^{-1}	4.79	4.81
Bandwidth, kHz	360–374	239
CF @ 6 mm gap, MHz	186.4	194.4

Advanced Photon Source

Setup Accelerator parameters, relevant to the APS measurements, are provided in Table 4. Since the Advanced Photon Source is not equipped with a longitudinal bunch-by-bunch feedback system, an improvised setup was created. A conventional front-end was used to detect the phase of the sum signal of a button position monitor relative to the 4th harmonic of the RF frequency. In the absence of a wideband longitudinal kicker we used an improvised kicker consisting of two transverse striplines driven common mode. The longitudinal shunt impedance of such a kicker has $\sin^2(\frac{\omega l}{2c})$ dependence on frequency [9]. For the APS striplines peak response occurs near $f_{\rm rf}/2$. Since nominal fill pattern populates every 4th RF bucket, we used the back-end shaper in iGp12 [10] to apply an inverted kick to the RF bucket following the bucket where the true kick was applied. The resulting modulation upconverts the kick to $f_{\rm rf}/2$, placing the kick signal near the peak of the stripline kicker's shunt impedance.

In our experiments we used two main types of streaming configurations:

- Four acquisition per mode, modes 1–323, roughly 11 minutes scan time;
- Ten acquisitions per mode, a subset of 48 modes, 4 minutes scan time.

The first measurement configuration covered all possible eigenmodes except the lowest frequency mode (mode 0). Based on several complete scans we have identified a subset of EFEMs with strong driving terms. These eigenmodes were then measured in more detail.

Individual measurements Figure 4 illustrates the time-domain evolution of two eigenmodes in a drive/damp measurement. Mode 36 was driven by the bunch-by-bunch feedback system to the initial level of 0.025° and decays exponentially in the 34 ms transient. At the same time, mode 0 is continuously excited by wideband and narrowband spectral

Table 4: APS Parameters

Parameter description	Value
Beam energy	7 GeV
Beam current	100 mA
Number of bunches	324
Nominal RF frequency	352 MHz
Harmonic number	1296
Synchrotron frequency	2.22 kHz
Radiation damping time	4.82 ms

ISBN: 978-3-95450-192-2 doi:10.18429/JACoW-IBIC2017-MO3AB1

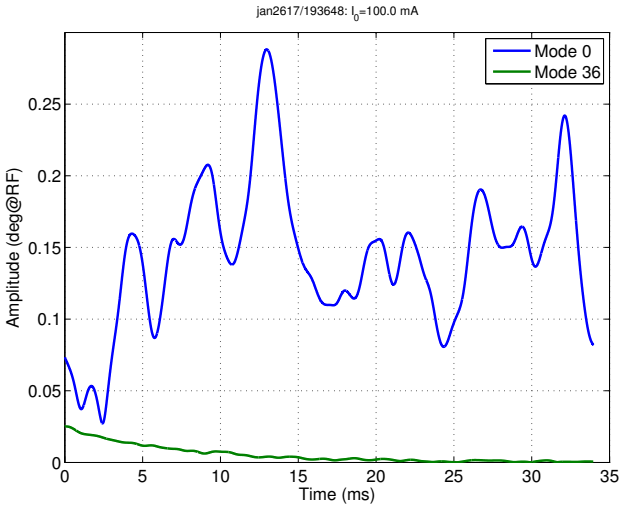

Figure 4: Time domain evolution of modes 0 (driven by RF disturbances) and 36 (excited by the LFB) in a drive/damp measurement at 100 mA.

components in the vicinity of the RF frequency to a much higher 0.14° average amplitude.

This significant difference between the externally driven motion of mode 0 and the achievable amplitudes of other modes points to the important machine setup requirement for these measurements. High degree of fill pattern uniformity is critical for successful measurements of this type. Variation in bunch currents multiplies the modal spectrum, producing a convolution in the frequency domain. Such convolution projects some of the motion of mode 0 to other modes, dramatically raising the measurement noise floor. Since the noise floor is typically on the order of 1.3 millidegrees, even small coupling from 140 millidegrees of mode 0 can compromise the signal of interest. The fill pattern uniformity requirement drops somewhat when a true longitudinal kicker is available, since much higher amplitudes can be reached.

Results of a single scan are shown in Fig. 5. The mode spectrum is folded around half the harmonic number h, to plot mirror modes l and $h-l$ (also denoted as $-l$) at the same point. The reason for that is that the coupling impedance function $Z(\omega)$ is hermitian, that is $Z(\omega) = Z^*(\omega)$ where * connotes complex conjugate [3, page 12]. As a result, eigenmodes l and $-l$ are driven by $Z(\omega)$ and $-Z^*(\omega)$, leading to identical imaginary part shifts (tune shifts) and opposing real part shifts (growth/damping rates). In such a presentation, narrowband resonances produce clearly visible shifts for pairs of modes, especially noticeable for modes 36, 151, and −95.

In order to tune the cavity HOMs we used cavity temperature control. In the APS, one can adjust cavity temperatures in sectors, with four cavities per sector. Both sector setpoint and individual cavity temperatures were recorded. Comparison of individual cavity temperatures to the setpoint shows a linear relationship in all cases. Thus, fitting and analysis

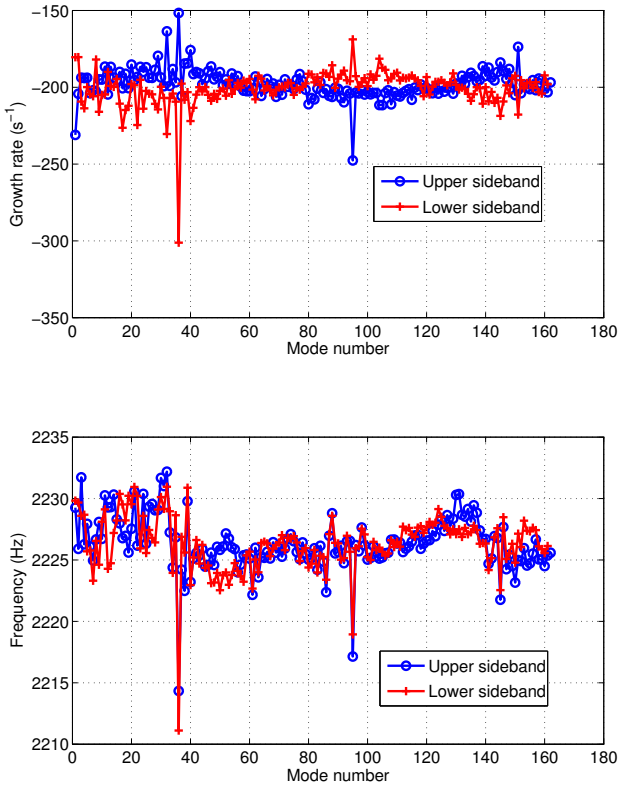

Figure 5: All mode scan at 76 mA. Modes 32, 36, 40, -95, 151 are clearly driven by narrowband resonances.

here were done relative to the sector setpoint rather than the temperature measurements of individual cavities.

HOM parameter fitting A set of modal scans taken at different temperature setpoints characterizes the dependence of all modal eigenvalues on that temperature. Many EFEMs do not respond to the temperature change. For those modes with significant eigenvalue shifts away from Λ_0, lack of response suggests the driving impedance is in a different RF sector. Mode −95 seen in Fig. 5 falls in that group. Later measurements showed that this mode is driven by cavity 4 in Sector 40. For modes without significant shifts from Λ_0, either there is no significant driving impedance or the resonant mode is tuned too far away from the relevant synchrotron sideband. Figure 6 shows the results of the temperature variation study in Sector 36. Eigenvalues of two modes, 36 and −36, are plotted versus temperature setpoint. The temperature scan was done at a beam current of 76 mA to keep the beam under the instability threshold. As Fig. 6 shows, mode 36 gets very close to the instability threshold at 82.5 °F.

The relationship between resonant frequency and temperature is assumed to be linear in the small temperature range explored in the experiment. For each HOM, we define

$$\omega_r(T) = \omega_{sb} + K_T(T - T_0) \quad (6)$$

Here ω_{sb} is the synchrotron sideband of the revolution harmonic to which the mode is tuned at temperature T_0.

ISBN: 978-3-95450-192-2 doi:10.18429/JACoW-IBIC2017-MO3AB1

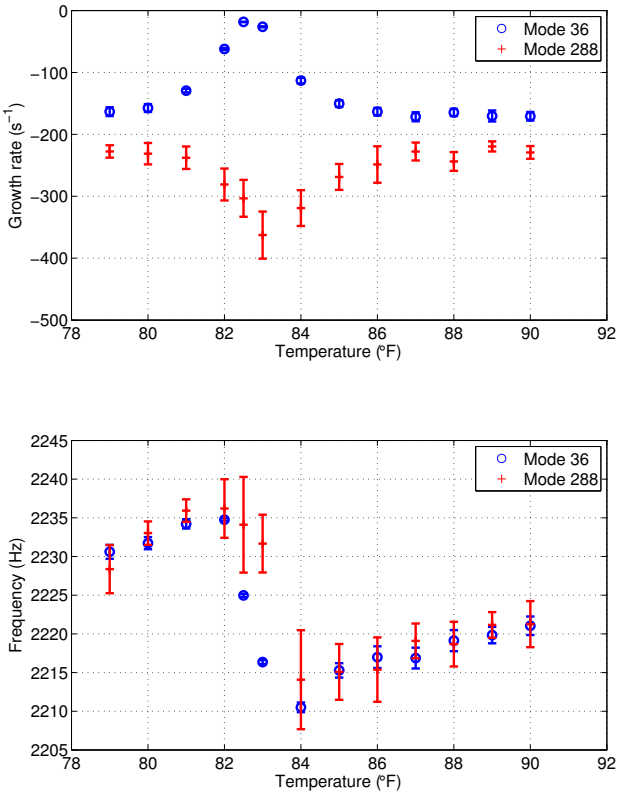

Figure 6: Modes 36 and 288(−36) are sampling the same HOM impedance.

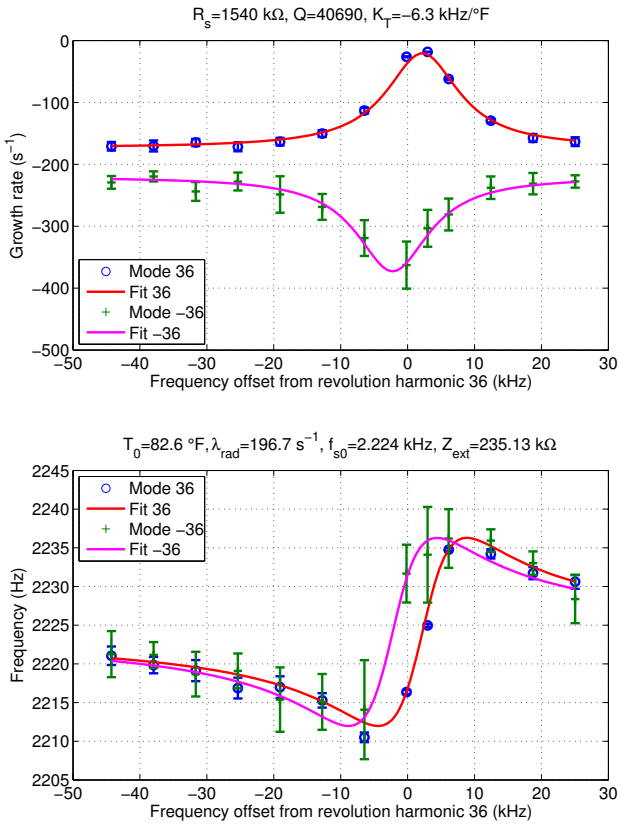

Figure 7: Fitting HOM response to both modes 36 and −36 extracts the temperature coefficient of the resonant mode. With known source frequency around 537 MHz the HOM is fully parameterized.

If we examine Fig. 6 carefully, we find a clear shift between peak growth rates for modes 36 and −36. Equations 1 and 2 help explain the asymmetry between positive and negative modes. That asymmetry is due to the fact that the positive mode samples the HOM impedance at $N\omega_{\mathrm{rf}} + M\omega_{\mathrm{rev}} + \omega_s$ while the negative mode reacts to the impedance at $-N\omega_{\mathrm{rf}} - M\omega_{\mathrm{rev}} + \omega_s$. As noted earlier, impedance function is hermitian, thus the negative mode is effectively sampling at $N\omega_{\mathrm{rf}} + M\omega_{\mathrm{rev}} - \omega_s$. Therefore, a separation of $2\omega_s$ can be used to extract the HOM temperature tuning sensitivity if the mode is narrow enough. From the plot, the difference between the two peaks is roughly 0.75 °F. That corresponds to $2f_s$ shift in the impedance center frequency, or 4.45 kHz. Dividing the two numbers we get the tuning sensitivity $K_T \approx 5.9$ kHz/°F.

Figure 7 shows the results of simultaneously fitting both modes 36 and −36. The estimated shunt impedance and Q are fairly close to the URMEL model predictions of 1.67 MΩ and 41,000, respectively. Extracted tuning sensitivity of 6.3 kHz/°F is in agreement with our rough estimate. Our earlier assumption of the linear relationship between temperature and HOM frequency is confirmed by the good agreement between measured and fitted eigenvalues.

Figure 8 illustrates one of the practical applications of this measurement. Plotting the fits to all the HOMs observed during the scan versus sector setpoint temperature gives us an easy way to optimize the operating temperature. Within the practically achievable range of setpoints from 80 to 90 °F minimum growth rate point is 87 °F. Since some variation of temperatures around the setpoint is to be expected, 86 °F is a slightly better practical choice.

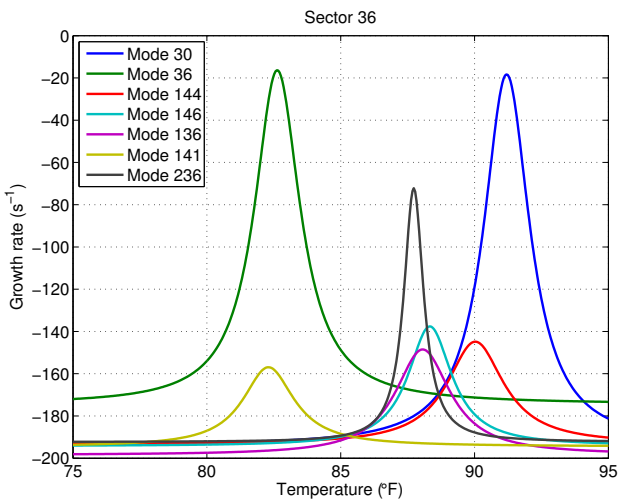

Figure 8: Growth rates due to all the HOMs observed in sector 36 at 74 mA.

ISBN: 978-3-95450-192-2 doi:10.18429/JACoW-IBIC2017-MO3AB1

Table 5: Rough identification of the HOMs

HOM frequency, MHz	537	918	1207
Cavity	Mode number		
S36C2	30	136	-98
S40C4	31	138	-95
S40C3	32	139	-92
S38C2	32	139	-91
S36C1	34	141	-88
S40C1	34	142	-86
S40C2	35	143	-83
S36C4	36	144	-82
S38C1	36	145	-80
S36C3	38	146	-77
S37C3	39	149	-72
S38C4	39	150	-71
S38C3	40	151	-69
S37C2	43	153	-63
S37C1	43	154	-61
S37C4	44	155	-59

After the APS upgrade (APS-U), the ring circumference will change slightly. As a result, to predict the minimum achievable growth rates with individual cavity temperature adjustments, we need to match the measured modes with the individual cavities. Table 5 provides a rough identification guide for three dominant HOMs in the APS cavities. This guide is generated as follows. With a single bunch in the ring to create a comb of revolution frequency harmonics, we examined individual cavity HOM probes, and for each mode recorded the revolution harmonic with the highest beam-induced power. Based on Table 5 we assign measured modes to individual cavities. For example, mode 36 measured during the Sector 36 temperature scan is assigned to cavity 4 in that sector. Resonance parameters, extracted from the fitting process, are then used to predict the APS-U growth rates at different cavity temperatures.

SUMMARY

New fourth-generation storage-ring based light sources are moving to beam parameters that make these accelerators more sensitive to driving impedances. In the longitudinal plane the sensitivity is enhanced by low synchrotron frequencies, with growth rates scaling as $1/\omega_s$. Transversely, this higher sensitivity comes about from the very low vertical emittances, with low emittance beams being more sensitive to residual dipole oscillations. Operation of bunch-by-bunch feedback systems at high loop gains, required to suppress fast growth rates, leads to higher residual motion amplitudes.

Precise characterization of resonant impedances becomes, therefore, more important for operational optimization, machine upgrades, and resonance mitigation. Beam-based techniques provide a powerful tool set for identifying and quantifying such resonances. Using multiple even-fill eigenmodes to sample the resonance we can extract shunt impedance, quality factor, center frequency (CF), and tuning sensitivity. In combination with modeling and single-bunch probing the effective impedances can be "unaliased".

These measurements can help provide much needed information prior to the installation of new insertion devices, changes in operating points, or major upgrades.

ACKNOWLEDGMENTS

For the studies at the Advanced Photon Source, special thanks to Nick Sereno, Ali Nassiri, and APS Controls and Operations staff. For the studies at the Australian Synchrotron we would like to thank Mark Atkinson, Mark Boland, Greg LeBlanc, Eugene Tan, Operations staff Louise Hearder and Madeleine Chalmers. Special thanks to Andrew Starritt and Andraz Pozar for software support. Thanks to Åke Andersson, David Olsson, Galina Skripka, Pedro Tavares, and MAX IV staff for their help with the measurements at the MAX IV 3 GeV ring.

REFERENCES

[1] S. Khan, *Collective phenomena in synchrotron radiation sources: Prediction, diagnostics, countermeasures*. Berlin: Springer, 2006.

[2] D. Teytelman *et al.*, "Accelerator diagnostic techniques using time-domain data from a bunch-by-bunch longitudinal feedback system," in *DIPAC 97: beam diagnostics and instrumentation for particle accelerators: Proceedings*, (Frascati (Rome) Italy), pp. 3–5, Laboratori Nazionali di Frascati: SIS–Pubblicazioni, 1997.

[3] D. Teytelman, *Architectures and algorithms for control and diagnostics of coupled-bunch instabilities in circular accelerators*. PhD thesis, Stanford University, 2003. SLAC-R-633.

[4] G. Rehm, M. Abbott, and A. Morgan, "New features and measurements using the upgraded transverse multibunch feedback at Diamond," in *Proceedings, 3rd International Beam Instrumentation Conference (IBIC2014) : Monterey, California, USA, September 14–18, 2014*, pp. 696–699, 2014.

[5] S. Prabhakar *et al.*, "Observation and modal analysis of coupled-bunch longitudinal instabilities via a digital feedback control system," *Part. Accel.*, vol. 57, p. 175, 1997.

[6] D. Teytelman, J. Fox, S. Prabhakar, and J. M. Byrd, "Characterization of longitudinal impedances in storage rings via multibunch effects," *Phys. Rev. ST Accel. Beams*, vol. 4, p. 112801, 2001.

[7] D. Olsson, L. Malmgren, and K. Åhnberg, "Design and implementation of stripline feedback kickers in the MAX IV 3 GeV storage ring," in *Proceedings, 8th International Particle Accelerator Conference (IPAC 2017): Copenhagen, Denmark, May 14-19, 2017*, pp. 4285–4288, 2017.

[8] J. Chi and D. Pelz, "Investigation of instability modes in 2-meter long in-vacuum undulator at the Australian Synchrotron," internal report, Australian Synchrotron, 2016.

[9] G. Lambertson, "Dynamic devices: Pickups and kickers," *AIP Conf. Proc.*, vol. 153, pp. 1413–1442, 1987.

[10] D. Teytelman, "Optimization of bunch-to-bunch isolation in instability feedback systems," in *Proceedings, 2nd International Beam Instrumentation Conference (IBIC2013): Oxford, United Kingdom, September 16–19, 2013*, pp. 116–119, 2013.